

# Propagation properties of photonic crystal fibers filled with nematic liquid crystals

T.R. WOLIŃSKI<sup>1</sup>, K. SZANIAWSKA<sup>\*1</sup>, K. BONDARCZUK<sup>1</sup>, P. LESIAK<sup>1</sup>, A.W. DOMAŃSKI<sup>1</sup>,  
R. DĄBROWSKI<sup>2</sup>, E. NOWINOWSKI-KRUSZELNICKI<sup>2</sup>, and J. WÓJCIK<sup>3</sup>

<sup>1</sup>Faculty of Physics, Warsaw University of Technology, 75 Koszykowa Str., 00–662, Warsaw, Poland

<sup>2</sup>Military University of Technology, 2 Kaliskiego Str., 00–908 Warsaw, Poland

<sup>3</sup>Maria Curie Skłodowska University, 5 M. Curie Skłodowskiej Sq., 20–031 Lublin, Poland

---

*The paper presents the latest experimental results on propagation properties of a photonic crystal fiber infilled with a nematic liquid crystal characterized by either extremely low (of the order of ~0.05) or relatively high (of the order of ~0.3) material birefringence. The nematic liquid crystal was introduced into the micro holes of the photonic crystal fiber by the capillary effect. Due to anisotropic properties of the obtained photonic liquid-crystal fiber, guiding mechanism that has to be attributed to the photonic band gap effect has been demonstrated.*

---

**Keywords:** liquid crystals, photonic band gap, optical fibers.

## 1. Introduction

Anisotropic optical fibers have been extensively investigated for over the last two decades [1]. This includes also liquid-crystal fibers with elliptical cores that reveal particular propagation and polarization properties as it has been recently demonstrated [2,3]. Another trend in liquid-crystal fiber research relies on exploiting microstructured photonic crystal fibers (PCFs) in which air holes are filled with liquid crystalline materials [4–6]. In this way we obtain a novel class of microstructured fibers that can be called photonic liquid-crystal fibers (PLCFs) [7,8].

Photonic crystal fibers are created as an array of silica tubs and rods, which are then heated to around 2000°C and drawn down to the fiber. The core is usually made by a defect in the periodical structure of the PCF cross-section; it can be missing or additional rod as well as capillary. In this way either hollow-core fibers or solid-core fibers are manufactured. Guiding of the light in a PCF is governed by one of two principal mechanisms responsible for light trapping within the core. The first is a simple propagation effect based on the total internal reflection (TIR) phenomenon, which is well known and similar to wave guiding within a conventional fiber. The other is known as a photonic band gap (PBG) effect that occurs when the averaged effective reflective index is lower in the core than in the cladding region. In this case, the guiding mechanism relies on the coherent backscattering of light into the core. The PBG guiding is usually met in hollow-core photonic crystal fibers.

When a nematic liquid crystal (LC) is introduced into a glass capillary, its molecular orientation strongly depends on capillary dimensions, boundary conditions, and on physical fields influencing the LC medium. Any external factor acting on the nematic core is in the position to change its effective refractive indices. The extraordinary index of refraction  $n_e$  depends on the angle  $\alpha$  between propagation direction and the optical axis and is described by

$$n_e(\alpha) = \frac{n_0 n_e}{\sqrt{n_0^2 \cos^2 \alpha + n_e^2 \sin^2 \alpha}}, \quad (1)$$

where  $n_0$  and  $n_e$  are the ordinary and extraordinary refractive indices, respectively.

## 2. Experimental

In this work, two different PCF host-structures (Fig. 1 and Table 1) were infilled with either low or highly birefringent nematic LC mixtures. The LC compositions included multicomponent esters mixtures composed at the Military University of Technology, Poland. Abbreviations for the materials used are P2 + 5%, 1550, 1600, and 12941B. Both ordinary  $n_0$  and extraordinary  $n_e$  refractive indices of the LC mixtures at a room temperature are presented in Table 2. Temperature dependences of refractive indices of the P2 + 5% liquid crystal material are shown in Fig. 4. Refractive indices of the highly birefringent LC mixture 1294 1B as a function of wavelength for 20 and 60°C are presented in Tables 3 and 4. For the 1600 and 1550 LC, there are specific temperature regions of the nematic phase (above 40°C, see Figs. 2 and 3) in which their ordinary refractive

\* e-mail: kasiaasz@if.pw.edu.pl

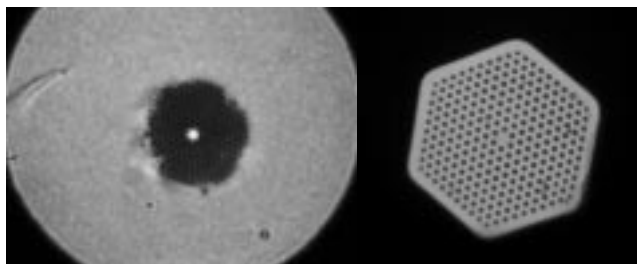


Fig. 1. Photonic crystal fibers to be filled with liquid crystals: 1006 structure (left-hand) and 1023 structure (right-hand).

indices  $n_0$  are below the refractive index of the fused silica  $n_{cl} = 1.458$  (at  $\lambda = 589$  nm) while the extraordinary indices are still higher than  $n_{cl}$ . Consequently, in this temperature region only single polarization could be guided within the fiber due to the TIR phenomenon.

Table 1. Parameters of the photonic crystal fibers used as host-structures.

PCF (cat. no.)	Hole diameter ( $\mu\text{m}$ )	Hole spacing ( $\mu\text{m}$ )
1006	0.7–1.0	2.0
1023	4.8	6.5

The best photonic crystal fiber to be filled with the nematic LC is the PCF with large holes that surround the solid core. The filling procedure is a time consuming process, e.g., preparing a sample of 20 cm long usually takes few days in the case of the PCF 1023 structure. Introducing a liquid crystal into the photonic crystal fiber with small holes (PCF 1006) requires much more time, at least two weeks.

### 2.1. Visible light propagation

To investigate spectral properties of the photonic crystal fibers, a prism spectrometer operating at the visible wavelengths (400–700 nm) was used. In the experiments, we measured both PCF structures filled with all types of LC mixtures presented in Table 2. Propagation properties of

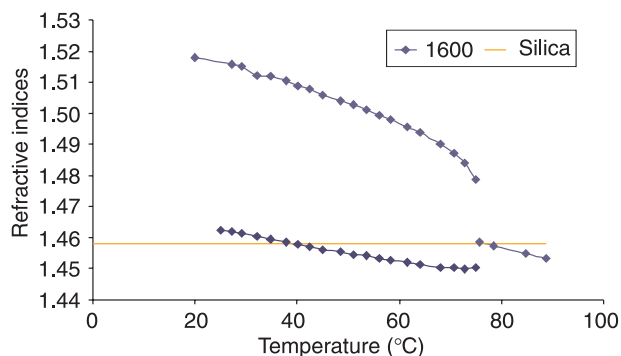


Fig. 2. Temperature dependences of refractive indices of the 1600 nematic LC mixture ( $\lambda = 589$  nm).

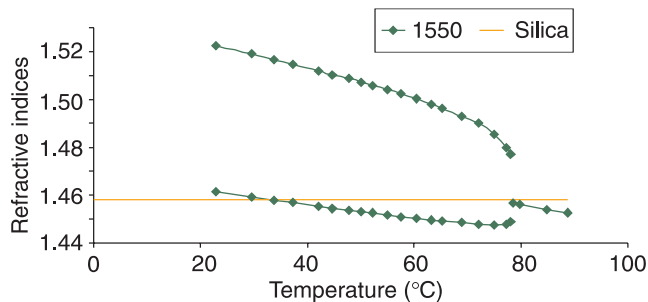


Fig. 3. Temperature dependences of refractive indices of the P2 + 5% nematic LC mixture ( $\lambda = 589$  nm).

the pure photonic crystal fiber and the PCFs infilled with liquid crystal were investigated in the experimental setup presented in Fig. 5, whereas a broad-band light source operating at the visible spectrum was used. The light was coupled to a short section of either the PCF or the manufactured PLCF.

Table 2. Birefringence of the nematic liquid crystals used as ghost materials (at room temperature,  $\lambda = 589$  nm).

LC mixture	Ordinary index $n_0$	Extraordinary index $n_e$	Birefringence $\Delta n$
P2 + 5%	1.458	1.500	0.042
1600	1.462	1.518	0.056
1550	1.461	1.522	0.061
1294 1B	1.501	1.813	0.312

Table 3. Refractive indices of 1294 1B LC mixture as a function of wavelength at the temperature 20°C ( $\lambda = 589$  nm).

Wavelength (nm)	20°		
	Ordinary index $n_0$	Extraordinary index $n_e$	Birefringence $\Delta n$
480	1.4974	1.8204	0.3230
589	1.5010	1.8130	0.3120
632.8	1.5040	1.8081	0.3041

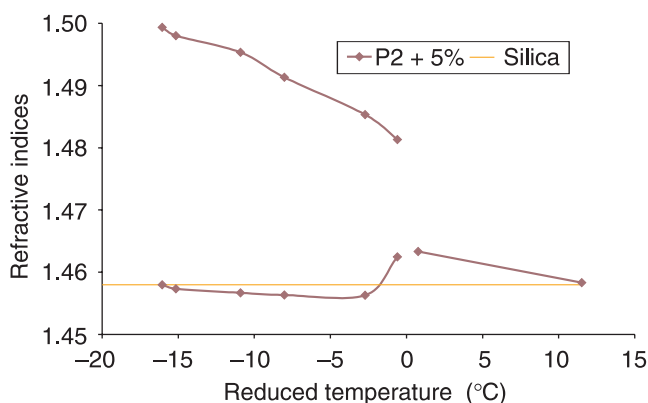


Fig. 4. Temperature dependences of refractive indices of the 1550LC nematic mixture ( $\lambda = 589$  nm).



Fig. 5. Experimental setup for investigation of propagation effects in empty and filled photonic crystal fibers.

Table 4. Refractive indices of 1294 1B LC mixture as a function of wavelength at the temperature of 60°C ( $\lambda = 589$  nm).

Wavelength (nm)	60°		
	Ordinary index $n_o$	Extraordinary index $n_e$	Birefringence $\Delta n$
480	1.4984	1.7877	0.2893
589	1.5011	1.7817	0.2806
632.8	1.5022	1.7776	0.2754

After launching a white light (at the visible wavelength range) into the 1006 and 1023 PCF structures, the whole visible spectrum at the output of the fiber was observed. However, when the same photonic crystal fiber was filled with any of the liquid crystal mixtures (Table 2), totally new propagation phenomena occurred.

In the PLCF composed of the 1023 PCF structure and one of two (either P2 + 5% or 1600) nematic LC mixtures we did not observe any propagation. It could be caused by either difficulties in the white light launching into the core region of the PCLF or by a strong attenuation at this wavelength region.

However, the PLCF consists of the 1023 PCF and the 1550 LC mixture could guide only a well-defined red spectral band (580–633 nm) from the whole visible wavelength range. Moreover, for the 1023 PCF filled with highly birefringent 12941B LC, only three selective wavelengths are being propagated (blue ~487 nm, green ~548 nm, and red ~607 nm).

This behaviour could be attributed to the appearance of the photonic band gap effect in the PLCF and can be explained as follows. The liquid crystalline material placed into the holes of cladding region is in the position to completely modify the guiding mechanism of such a micro-structured fiber. Light propagation within the solid-core photonic crystal fiber is based on the total internal reflection phenomenon and all the wavelengths are being transmitted. However, the guiding mechanism for the PLCF is based on the photonic band gap effect. The LC, characterized by a high birefringence that was introduced into the holes of the solid-core PCF reversed a sequence of the refractive indices, i.e., the PCF is characterized by the higher index of its core in comparison to the cladding region, whereas in the PLCF cladding has the higher refractive index than the core. In consequence, the PLCF propagates only selected wavelengths, depending on the LC molecular orientation within the holes.

An important feature of liquid crystals is their high sensitivity to external fields and perturbations. We have exam-

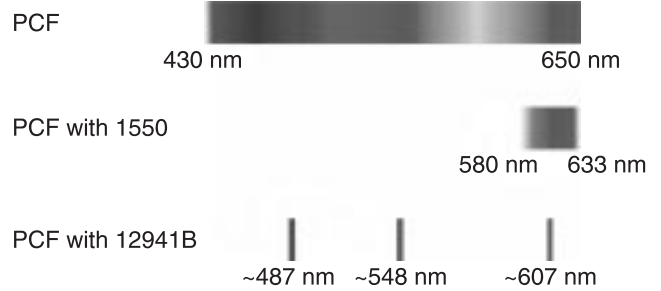


Fig. 6. Schematic representation of propagation effects in: 1023 PCF (upper), PLCF filled with low-birefringence 1550 liquid crystal (middle), and PLCF filled with high-birefringence 1294-1B liquid crystal (lower).

ined an influence of temperature and an external d.c. electrical field on propagation properties of the PLCF. The experimental setup is schematically presented in Fig. 7. After launching the light, exiting from a He-Ne laser to the 1006 PCF infilled with the 1550 nematic LC we observed light propagation at the red spectral band. The external electric field above a certain threshold value  $\sim 7$  V/ $\mu\text{m}$ , caused propagation decay within the PLCF that could be attributed to the well-known Frederiks transition (FT). FT usually occurs in LC structures with well-defined boundary conditions. Hence, it is evident that due to field-induced reorientation of LC molecules within the holes of the photonic liquid-crystal fiber different propagation mechanisms are possible.

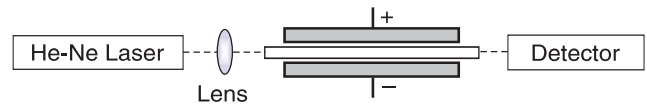


Fig. 7. Experimental setup to investigate influence of external electrical field on propagation properties of PLCF.

Moreover, temperature influence on propagation effects in the 1006 PCF filled with high-birefringence nematic LC (12941B) was investigated. For a white-light source no propagation was obtained at a room temperature. After heating, red light propagation appeared at the temperatures  $\sim 42.5^\circ\text{C}$  and  $\sim 38.2^\circ\text{C}$  by heating and cooling, respectively. The heating process was realized within the module, which is presented in Fig. 8.

## 2.2. Infrared light propagation

To investigate propagation effects in the PLCF for infrared light propagation (1500–1640 nm), we used the Tunicus Plus tunable laser source and the PAT 9000B polarimeter operating close to third telecommunication window and we measured the output power of the infrared light after the PLCF. For experimental investigation we used the 1006 photonic crystal fiber filled with both 1600 and P2 + 5% mixtures. These combinations of the PCF host-structure and the liquid crystal material were determined by setup re-

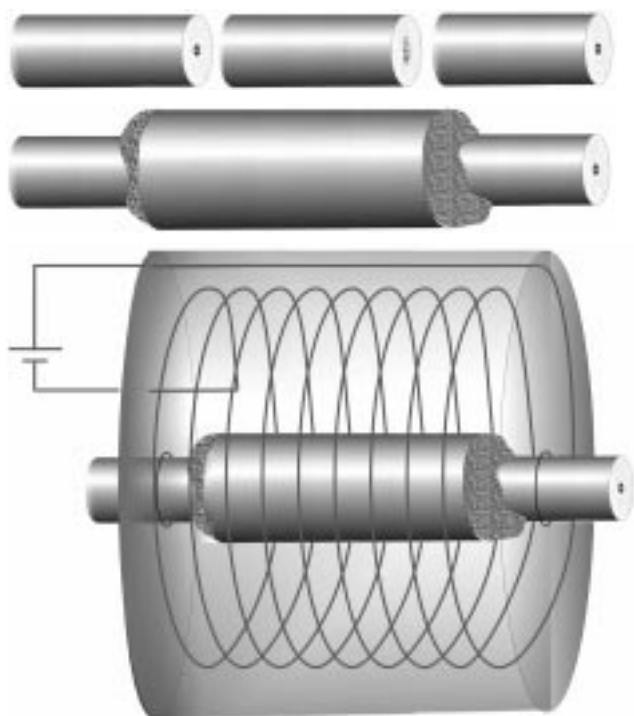


Fig. 8. Preparation of the sample: PLCF and leading telecommunication fibers (upper), PLCF housing (middle) and heating module (lower).

quirements. The tested PLCF was several centimeters long and connected to standard telecommunication fibers to lead in and out the coupled light (Fig. 8). We used face-to-face connectors between PLCF and telecommunication leading fibers surrounded by an external capillary with internal diameter equal to 127  $\mu\text{m}$ . Small size of the 1006 PCF core region (Table 2) enabled us light coupling between the PLCF and the leading fibers. The capillary with the PLCF was inserted into the heating module to measure influence of temperature on propagation properties of the PLCF.

### 3. Results and discussion

Results of the propagation effects in the PLCFs based on the 1006 host PCF are presented in Figs. 9 and 10. Figure 9 shows a comparison between propagation characteristics of the 1006 PCF (without LC) and of the PLCF filled with 1550 LC mixture. In the PLCF, propagation losses are in a certain region of wavelengths (1540–1580 nm) higher than in the pure 1006 PCF. However, the wavelength corresponding to the maximal attenuation in both PCF and PLCF is exactly the same. In this case the light is guided by photonic bandgap mechanism but we can observe only edges of the propagated wavelength band. Liquid crystal inserted into the holes of the photonic crystal fiber broadened the attenuation band and shifted the bandgap edge to the shorter wavelengths.

Figure 8 presents wavelength dependence of propagation losses in the PLCF filled with P2+5% mixture measured at selected temperatures. For low temperature value

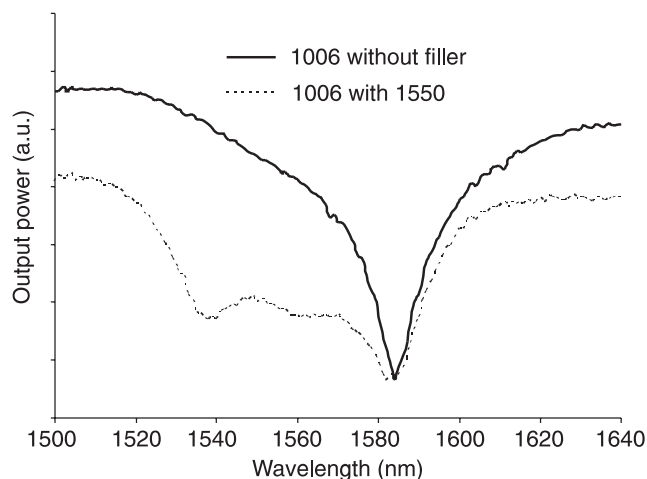


Fig. 9. Propagation losses in the 1006 PCF (without LC) and in the PLCF with the 1550 LC mixture at room temperature.

( $\sim 22.5^\circ\text{C}$ ) the optical output power has a local maximum close to 1550 nm. After heating we observed a slow shift of the output power local maximum towards the higher wavelengths. Moreover, other maximum appeared at  $31.1^\circ\text{C}$  where two maximums (around wavelengths: 1550 and 1575 nm) were observed. This wavelength dependence of the output power was very stable at a given temperature. This observation can be attributed to temperature tuning of the 1006 PCFs due to the presence of liquid crystal material within the microholes. To demonstrate subtle changes in propagation properties of the PLCF, the wavelength range shown in Fig. 8 was limited to 40 nm (1540–1580 nm).

However, by using a white light source, the PLCFs based on the 1023 PCF host structure exhibit totally different propagation behaviour. While the “empty” 1023 PCF guides the light by the modified total internal reflection mechanism, the same PCF filled with 1550 and 12941B liquid crystalline materials exhibits the photonic band gap

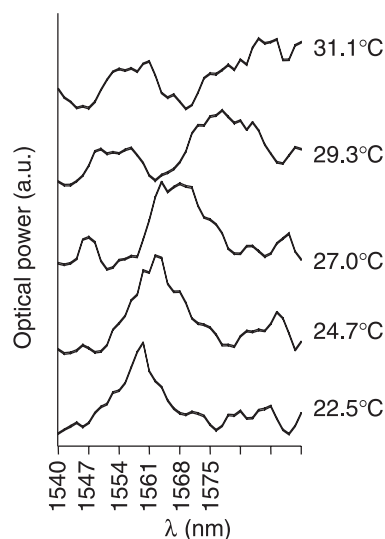


Fig. 10. Propagation losses in the 1006 PCF filled with P2-5% LC mixture measured at different temperatures.

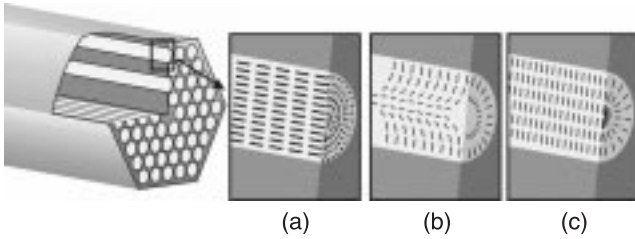


Fig. 11. Typical LC molecular arrangements within the holes of PCFs cladding region (a) planar, (b) axial, and (c) radial.

effect, at the output we observed propagation within the spectral band, 580–633 nm wavelengths for the 1550 PLCF and triple band-gap effect for the 12941B PLCF: selective blue (~487 nm), green (~548 nm), and red (~607 nm) light propagation, see Fig. 4. The propagation mechanism and especially the PBG effect strongly depend on molecular alignment within the host PCF holes as it is schematically drawn in Fig. 11.

The liquid crystalline molecular arrangement (director field configurations) in the cladding cylinders are determined by surface glass anchoring conditions. Generally, three types of alignment of the LC director inside the fiber’s holes are possible: planar [Fig. 11(a)], radial (homeotropic) [Fig. 11(c)], and a combination of two previous structures, the so-called radial-escaped or axial geometry [Fig. 9(b)]. Due to flow-induced orientation during the filling process planar and axial alignments dominate over the radial alignment.

According to the optical fibers theory, a photonic crystal fiber can be approximated by a step-index single-mode fiber and described by its core refractive index  $n_{co}$  and an average index of refraction of the hole-cladding  $n_{cl}$  that takes into account the holes region in the cladding.

Let us define a difference between core and the cladding refractive indices  $\Delta_i$ , where  $i = a, b, c$ , and  $d$  stand for the subcases:  $a$  is the “empty” PCF (without LC),  $b$  is the planar PLCF,  $c$  is the axial PLCF, and  $d$  is the radial PLCF (Fig. 10).

For the air-hole photonic crystal fiber [Fig. 12(a)] a difference between two refractive indices of the core and cladding regions is equal to  $\Delta_a$ . In the case of the planar alignment of LC molecules inside of the holes of cladding region, the value of  $\Delta_b$  decreases in comparison to the PCF

with air holes ( $\Delta_b < \Delta_a$ ) but the light is still being propagated by the total internal reflection mechanism [Fig. 12(b)]. It is a consequence of difference between air and LC ordinary refractive indices.

For the photonic liquid crystal fiber with axial configuration [Fig. 12(c)] various propagation effects can be observed. Since in this case the value of the indices difference  $\Delta_c \sim 0$  is very small depending on the molecular alignment fluctuations we can observe either weak propagation realized by the total internal reflection ( $n_{cl} < n_{co}$ ) or the photonic band gap ( $n_{cl} > n_{co}$ ) or even propagation disappearing ( $n_{cl} = n_{co}$ ).

For the radial structure [Fig. 12(d)], the difference between core and the cladding regions indices  $\Delta_d$  is negative and light propagation is only possible due to the photonic band-gap mechanism ( $n_{cl} > n_{co}$ ). Hence, in this case only selective wavelengths are being guided.

Depending on the type of LC material and the alignment of LC molecules inside cylindrical holes, different propagation effects were observed. From the classical total internal reflection mechanism with high and low indices contrasts to the photonic band-gap effect occurring for a wide range of the red wavelengths (around 50 nm) and also for three selective wavelengths (red, blue and green). Hence, LC molecular reorientation inside the cylindrical holes could influence light propagation in the PLCFs enabling a possibility for transition between both wave guiding mechanisms, from TIR to the tunable PBG mechanism. A summary of the experimental results is presented in Table 5 that exhibits guidance phenomena for various combinations of photonic crystal fibers and liquid crystals at both visible and infrared wavelengths ranges.

Table 5. Summary of the propagation mechanisms for various PCF and LC combination for visible and/or infrared wavelengths.

PCF \ LC	Air	P2 + 5%	1600	1550	1294 1B
1006	TIR(vis)/ PBG(ir)	PBG (ir)	PBG (ir)	PBG (vis/ir)	PBG (vis)
1023	TIR (vis)	-(vis)	-(vis)	PBG (vis)	PBG (vis)

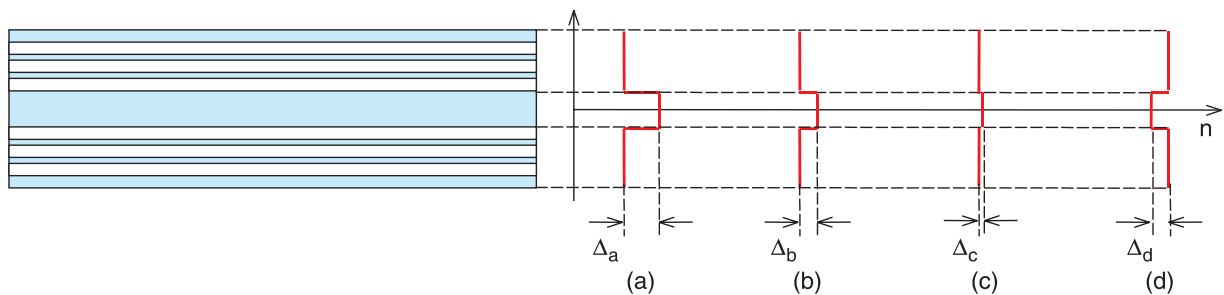


Fig. 12. Influence of LC molecular arrangements within the holes on the contrast between core and cladding refractive indices: (a) PCF without LC; (b) planar, (c) axial, and (d) radial structure of LC within the PLCF.

## 4. Conclusions

We have demonstrated propagation effects in PLCFs composed of PCFs infilled with both low and highly birefringent nematic LC mixtures. The main advantage of the microstructured PLCFs relies in their tuning possibilities and abilities to modify propagation properties of the PLCFs. Depending on the LC materials introduced into photonic crystal fibers switching between two propagation mechanisms, total internal reflection and photonic band gap can be realized. Also electrically and temperature-induced tuning of light propagation in PLCFs was demonstrated.

## Acknowledgements

This work was partially supported by the Warsaw University of Technology and by the Polish State Committee for Scientific Research.

## References

1. T. R. Woliński, "Polarimetric optical fibers and sensors", in *Progress in Optics*, Vol. 40, pp. 1–75, edited by E. Wolf, North-Holland, Amsterdam, 2000.
2. T.R. Woliński, "Polarization phenomena in optical systems", in *Encyclopaedia of Optical Engineering*, pp. 2150–2175, edited by R.G. Diggers, Marcel Dekker Inc., New York, 2003.
3. T.R. Woliński, P. Lesiak, R. Dąbrowski, J. Kędzierski, and E. Nowinowski-Kruszelnicki, "Polarization mode dispersion in an elliptical liquid crystal-core fiber", *Mol. Cryst. Liq. Cryst.* **421**, 175–186 (2004).
4. T.T. Larsen, A. Bjarklev, D.S. Hermann, and J. Broeng, "Optical devices based on liquid crystal photonic bandgap", *Optics Express* **11**, 2589–2596 (2003).
5. T.T. Alkeskojld, L.A. Bjarklev, D.S. Hermann, Anawati, J. Broeng, J. Li, and S.T. Wu, "All-optical modulation in dye-doped nematic liquid crystal photonic bandgap fibers", *Optics Express* **12**, 5857–5871 (2004).
6. R. Kotynski, M. Antkowiak, H. Thienpont, and K. Panajotov, "Modelling of polarization behaviour of LC filled photonic crystal fibers", in *Proc. Symp. IEEE/LEOS Benelux Chapter*, 2004, Ghent, Belgium, 315–331 (2004).
7. J.A. Reyes-Cervantes, J.A. Reyes-Avandano, and P. Helevi, "Electrical tuning of photonics crystal infilled with liquid crystal", *Proc. SPIE* **5511**, 50–60 (2004).
8. T.R. Woliński, K. Bondarczuk, K. Szaniawska, and P. Lesiak, "Propagation effects in photonic crystal fiber filled with a low-birefringent liquid crystal", *Proc. SPIE* **5518**, 232–237 (2004).